The exported chaperone PfHsp70x is dispensable for the *Plasmodium falciparum* intraerythrocytic lifecycle.

David W. Cobb*[1], Anat Florentin*[1,2], Michelle Krakowiak[1], Vasant Muralidharan[#,1,2]

[1] Department of Cell Biology

[2] Center for Tropical and Emerging Global Diseases

University of Georgia, Athens, Georgia, United States of America

*These authors contributed equally to this work.

[#] Corresponding author: vasant@uga.edu

Abstract

Export of parasite proteins into the host erythrocyte is essential for survival of *Plasmodium falciparum* during its asexual lifecycle. While several studies described key factors within the parasite that are involved in protein export, the mechanisms employed to traffic exported proteins within the host cell are currently unknown. Members of the Hsp70 family of chaperones, together with their Hsp40 co-chaperones, facilitate protein trafficking in other organisms, and are thus likely used by *P. falciparum* in the trafficking of its exported proteins. A large group of Hsp40 proteins is encoded by the parasite and exported to the host cell, but only one Hsp70, PfHsp70x, is exported with them. PfHsp70x is absent from most *Plasmodium* species and is found only in *P. falciparum* and closely-related species that infect Apes. Herein, we have utilized CRISPR/Cas9 genome editing in *P. falciparum* to investigate the essentiality of PfHsp70x. We show that parasitic growth was unaffected by knockdown of PfHsp70x using both the DHFR-based Destabilization Domain and the *glmS* ribozyme system. Similarly, a complete gene knockout of PfHsp70x did not affect the ability of *P. falciparum* to proceed through its intraerythrocytic lifecycle. The effect of PfHsp70x knockout on the export of proteins to the host RBC was tested and we found that this process was unaffected. These data show that although PfHsp70x is the sole exported Hsp70, it is not essential for the asexual development of *P. falciparum*.

Importance

Half of the world's population lives at risk for malaria. The intraerythrocytic lifecycle of *Plasmodium* spp. is directly responsible for clinical manifestations of malaria; therefore,

detailed knowledge of the parasite's ability to survive within the red blood cell is needed to combat the deadliest agent of malaria, *P. falciparum*. An outstanding question in the field is how *P. falciparum* undertakes the essential process of trafficking its proteins within the host. In most organisms, chaperones such as Hsp70 are employed in protein trafficking. The chaperone PfHsp70x is unique to *P. falciparum,* and it is the only parasite protein of its kind exported to the host. This has placed PfHsp70x as an ideal target to inhibit protein trafficking and kill the parasite. Here we show that, despite earlier notion, PfHsp70x is not required for export of parasite effectors to the host nor is it essential for parasite survival inside of the RBC.

Introduction

Malaria is a profound killer worldwide. In 2015, 214 million cases of malaria resulted in 438,000 deaths, largely in Africa and Asia (1). Within malaria endemic countries, the disease targets the most vulnerable of the population, including children under five and pregnant women (1). The disease is caused by infection with eukaryotic parasites from the genus *Plasmodium*, but it is one species—*P. falciparum*—that is responsible for most of the malaria associated mortality. The clinical manifestations of malaria range from fever, headache, and muscle pains, to severe anemia, coma, and respiratory distress (2). All of these symptoms are direct consequences of asexual replication of the parasite within the human red blood cell (RBC)(3). During this cycle of replication, *P. falciparum* invades the RBC and dramatically transforms its morphology and physiology. Alterations to the RBC include increased permeability, loss of cell deformability, and introduction of virulence-associated knobs at the RBC membrane (4, 5).

60

61 Remodeling of the RBC requires export of hundreds of parasite proteins into the host
62 cell, a feat involving protein trafficking through multiple compartments before arriving at
63 their final destinations in the host. The first phase of the journey begins in the parasite
64 endoplasmic reticulum (ER). Many exported proteins contain an N-terminal signal motif
65 termed the Host Targeting Signal or *Plasmodium* Export Element (PEXEL) (6, 7). A key
66 step in the export of PEXEL-containing proteins is cleavage of the motif by the ER-
67 resident aspartyl protease Plasmepsin V (8–10). A sub-group of exported proteins
68 called PEXEL-Negative Exported Proteins (PNEPs) lack the motif, but their N-terminus
69 is similarily necessary for export (11, 12). Aside from Plasmepsin V processing of
70 PEXEL, mechanisms underlying the selection of host-destined proteins for exit from the
71 ER remain unclear. Nonetheless, PEXEL-proteins and PNEPs continue their journey
72 through the parasite's secretory pathway and are delivered to the parasitophorous
73 vacuole (PV), a membranous structure within which the parasite resides. Previous
74 studies have shown that proteins cross the parasitophorous vacuole membrane (PVM)
75 through the *Plasmodium* Translocon of Exported Proteins (PTEX) (13–15) . Once they
76 are on the other side of the PVM, all classes of proteins need to refold and find their
77 specific subcellular localization, whether it is in the host cytoplasm, the host membrane,
78 or parasite-induced structures such as knobs or Maurer's clefts. It is completely
79 unknown how hundreds of proteins, within a short time period, cross through PTEX,
80 refold to regain structure and function, and find their final destination in the host.
81

82 The process of protein export is essential for *P. falciparum* survival in the RBC, as
83 blockage of protein export—whether at the parasite ER or at the PVM—results in
84 parasite death. In the ER, overexpression of catalytically dead PMV results in impaired
85 parasite growth, and inhibition of PMV with a PEXEL-mimetic impairs protein export and
86 kills parasites during the transition to the trophozoite stage (9, 16, 17). Similarly, *P.*
87 *falciparum* parasites are sensitive to interference of trafficking across the PVM.
88 Conditional knockdown of PTEX components blocks protein export and kills the
89 parasites (18, 19). As the parasites are susceptible to inhibition of trafficking in the ER
90 and PV, interference in the trafficking process within the host may similarly impair
91 parasite growth. The mechanisms of protein trafficking inside of the host cell remain
92 unknown, but identification of essential components of this process will provide valuable
93 targets for drug discovery programs.
94
95 Molecular chaperones are likely candidates in the search for key export and trafficking
96 components. Indeed, PfHsp101 is an essential component of PTEX, and its inhibition
97 results in accumulation of exported proteins within the PV (18). Furthermore, several
98 parasite Hsp40s are exported to the RBC, but their function there is unknown (20). In
99 other organisms Hsp40s serve as co-chaperones for Hsp70s , but in contrast to the
100 large number of exported Hsp40s, PfHsp70x (PF3D7_0831700) is the only parasite-
101 encoded Hsp70 that is exported to host cell (21, 22). This chaperone is found only in *P.*
102 *falciparum* and not in other *Plasmodium* species that infect humans, such as *P. vivax* or
103 *P. knowlesi* (21). Within the *P. falciparum* infected RBC, PfHsp70x is localized to the PV
104 and the host, where it associates with PfHsp40s in mobile structures termed J-dots (21).

105 Given its status as sole exported Hsp70, we hypothesized that PfHsp70x is central to
106 protein trafficking in the host cell, and thus essential to parasite viability. Indeed, studies
107 focused on PTEX interactions have found PfHsp70x associated with the translocon, and
108 it has been shown to co-localize with the critical virulence protein PfEMP1 during its
109 trafficking (21, 23, 24).
110
111 In this study, we took advantage of various genetic tecniques to show that PfHsp70x is
112 non-essential for protein export and parasite growth. We have used the DHFR-based
113 destabilizing domain that has previously been used to inhibit chaperone function (18,
114 25). In addition, we have used the *glmS*-ribozyme system that inhibits translation via
115 mRNA degradation (26). Both methods were succesful in either reducing protein levels
116 or function but had no impact on protein export or parasite growth. To confirm that the
117 lack of a phenotype was not due to incomplete knockdown, we used CRISPR/Cas9
118 technology to generate a complete knockout of the PfHsp70x gene and found no
119 defects in parasite proliferation. Our data demonstrate that PfHsp70x is not required for
120 protein export to the host RBC and not essential for the intraerythrocytic lifecycle of *P.*
121 *falciparum*.
122
123 **Results and Discussion**
124 **Conditional inhibition of PfHsp70x activity using the DHFR-based Destabilization**
125 **Domain.** Previous work has shown that chaperones fused to a DHFR-based
126 destabilization domain (DDD) are auto-inhibited when the DDD is in its unfolded state
127 (18, 25), unlike other proteins which are degraded when fused to the DDD (27–29). In

128 the presence of the stabilizing ligand trimethoprim (TMP), the DDD is folded and the
129 chaperone functions normally. However, upon TMP removal the DDD is unfolded and
130 binds to its attached chaperone intramolecularly, thereby blocking interactions with the
131 chaperone's client proteins and inhibiting normal chaperone function (**Fig. 1A**). Relying
132 on a single-crossover homologous recombination, the *pfhsp70x* gene was modified with
133 a triple-HA tag and the DDD, and integration at the *pfhsp70x* locus was confirmed via
134 Southern blot analysis (**Fig. 1A, B**). Consistent with the auto-inhibitory model of
135 chaperone-DDD action, western blot analysis of parasite lysates following TMP removal
136 showed that PfHsp70x protein levels remain consistent over time (**Fig. 1C**). Isolation of
137 the host cell cytoplasm using saponin lysis revealed that PfHsp70x-DDD is exported to
138 the host cell. Moreover, the persistence of PfHsp70x in the supernatant following TMP
139 removal indicated that PfHsp70x is exported to the host cell even in its putative inhibited
140 form. To assess the role of PfHsp70x in parasite proliferation, we removed TMP and
141 measured asexual growth over a course of several days and at least two replication
142 cycles. We found that the absence of TMP had no effect on parasite proliferation (**Fig.
143 2A**). It was previously reported that PfHsp70x , together with several other exported
144 chaperones, localizes to specific punctate structures in the host cell termed J-dots. To
145 test the effect of DDD-based inhibition on PfHsp70x localization, we performed
146 immunofluorescence assays and found that PfHsp70x-DDD is trafficked to the expected
147 punctate structures within the host cell, regardless of TMP presence (**Fig. 2B**). These
148 data suggest that inhibition of PfHsp70x activity using the DDD system does not affect
149 the asexual life cycle of the parasite. Nevertheless, we could not assess the degree of
150 inhibition and therefore could not exclude the possibility that the chaperone activity was

151 unaffected by the DDD fusion, leading to the lack of a growth phenotype. We therefore
152 utilized alternative methods to reduce PfHsp70x protein levels in the parasite.
153
154 **Conditional Knockdown of PfHsp70x Using the *glmS* Ribozyme.** Next, we sought to
155 conditionally knockdown PfHsp70x at the mRNA level using the *glmS* ribozyme (26). In
156 this system, the *glmS* ribozyme sequence is inserted into the 3' end of the genomic
157 locus of a gene and is transcribed with the gene as one mRNA. Addition of the small
158 molecule glucosamine (GlcN) activates the *glmS* ribozyme, which cleaves itself from the
159 mRNA, disconnecting the transcript form its polyA tail and leading to its degradation
160 (**Fig. 3A**). Using CRISPR/Cas9 genome engineering, we appended a triple HA tag to
161 the C-terminus of PfHsp70x followed by the *glmS* ribozyme (**Fig. 3A**) (30). A second cell
162 line was generated in which the *pfhsp70x* locus was tagged with a mutant version of the
163 ribozyme—termed *M9*—which is unresponsive to GlcN and serves as a control during
164 GlcN treatment. Following transfection and drug selection, PfHsp70x-*glmS* and
165 PfHsp70x-*M9* clones were isolated via limiting dilution. PCR analysis revealed the
166 correct integration of the tag and ribozyme into the *pfhsp70x* gene in all clonal parasite
167 lines (**Fig. 3B**). Additionally, immunofluorescence assays confirmed that PfHsp70x-
168 *glmS* is exported to the host cytoplasm, where it is found, as before, in punctate
169 structures that are distinct from Maurer's clefts, suggestive of J-dot localization (**Fig.
170 3C**).
171
172 Next, we tested the effect of reducing PfHsp70x levels on intraerythrocytic growth. To
173 ensure that insertion of the ribozyme itself does not interfere with normal asexual

174 growth, PfHsp70x-*glmS*, PfHsp70x-*M9*, and the parental line (3D7) were grown in the
175 absence of GlcN. Indeed, we found that in the absence of GlcN, growth of both the
176 *glmS* and *M9* cell lines was comparable to 3D7 (**Fig. 4A**). Next, PfHsp70x-*glmS* and
177 PfHsp70x-*M9* were cultured with GlcN and parasitemia was measured via flow
178 cytometry. The growth of PfHsp70x-*glmS* and PfHsp70x-*M9* was unaffected by
179 treatment with 5 mM and 10 mM GlcN (**Fig. 4B**). To confirm that PfHsp70x protein level
180 is reduced in response to GlcN, schizont-stage parasites from the *glmS* and *M9* cell
181 lines were Percoll-purified and whole parasite lysates were used for western blotting.
182 Using anti-HA antibody we found that treatment with GlcN reduced protein levels in
183 PfHsp70x-*glmS* but did not affect protein levels in PfHsp70x-*M9* (**Fig. 4C**). Together,
184 these data show that we can efficiently reduce PfHsp70x levels using the *glmS*
185 ribozyme but this has no affect on the asexual growth of the parasite within the RBC.
186
187 **Knockout of *pfhsp70x* does not affect parasite growth**. We successfully utilized two
188 different conditional knockdown approaches to modify PfHsp70x activity and
189 expression, but these knockdowns were insufficient to produce a growth defect in the
190 parasites. Therefore, we sought to definitively test the essentiality of PfHsp70x via
191 complete genomic knockout (termed PfHsp70x-KO). To this end, we employed
192 CRISPR/Cas9 to interrupt the PfHsp70x ORF by inserting a human dihydrofolate
193 reductase (*hdhfr*) drug resistance cassette (**Fig. 5A**). Following transfection and
194 selection with WR99210, PfHsp70x-KO parasites were cloned via limiting dilution.
195 Southern blot analysis of genomic DNA isolated from the parental line and independent
196 clones showed that the *hdhfr* cassette was inserted into the *pfhsp70x* gene via

197 homology directed repair (**Fig. 5B**). To verify that the null mutants do not express
198 PfHsp70x, schizont-stage parasites from two independent knockout clones and the
199 parental line were Percoll-purified, and whole parasite lysates were used for western
200 blotting. Probing with anti-PfHsp70x shows that the knockout clones do not express
201 PfHsp70x (**Fig. 5C**). Finally, intraerythrocytic growth of the PfHsp70x-KO clones was
202 monitored over two replication cycles. In agreement with the lack of any growth
203 phenotype in the conditional knockdown parasite lines, the PfHsp70x-KO parasites
204 displayed *wild-type* level of proliferation in erythrocytes (**Fig. 5D**). The normal growth in
205 the complete absence of PfHsp70x expression conclusively demonstrates that
206 PfHsp70x activity is not essential for the asexual growth of the parasite within the RBC.
207
208 **Protein export is unimpaired in PfHsp70x-KO parasites**. Although PfHsp70x is
209 dispensible for the intraerythrocytic lifecycle in culture, we reasoned that it could
210 nonetheless play a role in export of proteins to the host cell. In particular, we
211 hypothesized that PfHsp70x is needed for the export of proteins known to mediate
212 virulence of *P. falciparum* infection, as trafficking defects of these proteins would not
213 manifest as arrest of the asexual lifecycle (20). Using immunofluorescence, we
214 examined localization of specific virulence-associated proteins in 3D7 and PfHsp70x-
215 KO. First, the localization of the PEXEL-containing PfFIKK4.2, an exported kinase
216 associated with knob formation and infected RBC rigidity (31), is unchanged in
217 PfHsp70x-KO parasites **(Fig. 6A)**. Next, we examined the localization of the PEXEL-
218 containing protein KAHRP, which is essential for the formation of knobs on the surface
219 of infected RBCs (32). Export of this protein was not inhibited in PfHsp70x-KO parasites

220 **(Fig. 6B)**. Finally, we determined the localization of the PNEP MAHRP1, which has
221 been implicated in PfEMP1 presentation at the RBC surface (33), and found that its
222 export is not impaired by the absence of PfHsp70x **(Fig. 6C)**. These data show that the
223 loss of PfHsp70x does not impede the parasite's ability to export virulence-associated
224 proteins to the host cell.
225
226 Even though PfHsp70x is the only parasite-encoded Hsp70 that is exported to the RBC,
227 our results demonstrate that it is not required for intraerythrocytic growth. However,
228 PfHsp70x is not the only Hsp70 found in infected RBCs. Human Hsp70 is present in the
229 erythrocyte cytoplasm (34). Thus, the role played by PfHsp70x in the parasite's biology
230 could be redundant with the human Hsp70 that is already present in the host cell. In
231 fact, infection with *P. falciparum* affects the normal localization of the human Hsp70, as
232 the protein is soluble in non-parasitized RBCs but is found in detergent-resistant
233 fractions following infection (35). The methods used here to investigate the function of
234 PfHsp70x, knockdown and complete genomic knockout, are more challenging to use for
235 human Hsp70. The mature RBC cannot be genetically manipulated, and knockdown of
236 human Hsp70 in hematopoietic stem cells abrogates RBC formation (36). Furthermore,
237 detailed analysis of the *pfhsp70x* locus in strains isolated from the field may be
238 informative about the essentiality of PfHsp70x in human infections. Overall, our data
239 demonstrate that PfHsp70x is not required for export of *P. falciparum* effector proteins
240 to the host and is dispensible for asexual growth within human RBCs.
241
242

243

244 **Materials and Methods**

245 **Plasmid construction.** Genomic DNA was isolated from *P. falciparum* using the
246 QIAamp DNA blood kit (QIAGEN). Constructs utilized in this study were confirmed by
247 sequencing. PCR products were inserted into the respective plasmids using the In-
248 Fusion cloning system (Clonetech) or using the SLIC method. Briefly, insert and cut
249 vector were mixed with a T4 DNA polymerase and incubated for 2.5 minutes at room
250 temperature, followed by 10 minutes incubation on ice and then transformed into
251 bacteria. For generation of plasmid PfHsp70x-HADB, a 1-kb homologous sequence
252 from the 3'-end of the *pfhsp70x* gene (not including the stop codon) was amplified by
253 PCR using primers 5'-
254 CACTATAGAACTCGAGGTGAAAAAGCTAAACGTGTATTATCATCATCCGCACAAGC-
255 3' and 5'-
256 CGTATGGGTACCTAGGATTTACTTCTTCAACGGTTGGTCCATTATTTTGTGC-3' and
257 was inserted into pHADB (18) using restriction sites XhoI and AvrII (New England
258 Biolabs).

259

260 For the generation of the *glmS* conditional mutants three plasmids were used; 1) pUF1-
261 Cas9 (from J. J. Lopez-Rubio) was used to drive cas9 expression (30). 2) pMK-U6 was
262 used to drive expression of the RNA guide. For this purpose, pL6 plasmid (from J. J.
263 Lopez-Rubio, (30)) was digested with NotI and NcoI (New England Biolabs) and the
264 fragment that contained the U6 RNA expression cassette was blunted and re-ligated to
265 form the pMK-U6 plasmid. The guideRNA, oligos 5'-

266 TAAGTATATAATATTTGCATTATTGTTGTATATTTGTTTTAGAGCTAGAA-3' and 5'-
267 TTCTAGCTCTAAAACAAATATACAACAATAATGCAAATATTATATACTTA-3' were
268 annealed and cloned into the RNA module in MK-U6 as previously described (30).
269 Briefly, pMK-U6 was digested with BtgZI (New England Biolabs) and annealed oligos
270 were inserted using In-Fusion HD Cloning Kit (Clontech). 3) pHA-glmS and pHA-M9
271 were used as donor DNA templates consisting of two homology regions flanking the HA
272 tag and the *glmS* (or the *M9*) sequences. To generate the pHA-glmS and pHA-M9
273 plasmids, primers 5'-
274 GAGCTCGCTAGCAAGCTTGCCGGCAAGATCATGTGATTTCTCTTTGTTCAAGGAGT
275 C-3' and 5'-
276 TCCGCGGAGCGCTACTAGTTACCCATACGATGTTCCAGATTACGCTTACCCATACG
277 ATGTTCCAGATTACGCTTACCCATACGATGTTCCAGATTACGCTTAAATGTCCAGAC
278 CTGCAGTAATTATCCCGCCCGAACTAAGCGC-3' were used to amplify the *glmS* and
279 *M9* sequences from pGFP-glmS and pGFP-M9, respectively (from P.Shaw, (26)). PCR
280 constructs were then inserted into a TOPO cloning vector (ThermoFisher). To allow
281 efficient genomic integration of the pHA-glmS and pHA-M9 donor plasmids, 800bp
282 sequences were used for each homology region. The C-terminus of the *pfhsp70x*
283 coding region was PCR amplified form genomic DNA using primers 5'-
284 AATTCGCCCTTCCGCGGGCTGTACAAGCAGCCATCTTATCAGGTGATCAATCATC-
285 3' and 5'-
286 ATCGTATGGGTAAGCGCTATTTACTTCTTCAACGGTTGGTCCATTATTTTGTGCTTC-
287 3' and was inserted into pHA-glmS and pHA-M9 using restriction sites SacII and AfeI
288 (New England Biolabs). The 3'UTR of *pfhsp70x* was pcr amplified from genomic DNA

289 using primers 5'-
290 ATGATCTTGCCGGCAAGCTTACGAAAATATACAACAATAATGCATAAAATAATAATA
291 ATT-3' and 5'-
292 CCTTGAGCTCGCTAGCGCAATATAAATGGATTATTCCTTTTGTATATAATTTAAAATA
293 AG-3' and was inserted into pHA-glmS and pHA-M9 (already containing the C-terminus
294 homology region) using restriction sites HindIII and NheI (New England Biolabs).
295 For the generation of *pfhsp70x-ko* parasites two plasmids were used; 1) A cas9
296 expressing plasmid (as described above), and 2) pL7-PfHsp70x plasmid that is derived
297 from the pL6 plasmid (from J. J. Lopez-Rubio, (30)). pL7-PfHsp70x contained the guide
298 RNA and 800bp homology regions flanking a *hdhfr* gene that confers resistance to WR.
299 The N-terminus of the *pfhsp70x* gene was amplified via PCR from genomic DNA using
300 primers 5'- cggggaggactagtATGAAGACAAAAATTTGTAGTTATATTCATTATATTG-3'
301 and 5'- acaaaatgcttaagGGAAACATCTTTACCTCCATTTTTTTTTTTAAAATCTTGTAC-3'
302 and was inserted into pL6 using restriction sites AflII and SpeI (New England Biolabs).
303 The C-terminus of the *pfhsp70x* gene was pcr amplified from genomic DNA using
304 primers 5'-
305 taaatctagaattcTGATCAATCATCAGCTGTCAAAGACTTATTATTATTAGATG-3' and 5'-
306 ttaccgttccatggTTAATTTACTTCTTCAACGGTTGGTCCATTATTTTGTGCTTC-3' and
307 was inserted into pL6 (already containing the C-terminus homology region) using
308 restriction sites NcoI and EcoRI (New England Biolabs). In order to insert the guide
309 DNA sequence, oligos 5'-
310 TAAGTATATAATATTGTACAAGCAGCCATCTTATCGTTTTAGAGCTAGAA-3' and 5'-
311 TTCTAGCTCTAAAACGATAAGATGGCTGCTTGTACAATATTATATACTTA-3' were

312 annealed and cloned into pL6 as previously described (30). Briefly, pL6 was digested
313 with BtgZI (New England Biolabs) and annealed oligos were inserted using In-Fusion
314 HD Cloning Kit (Clontech).
315
316 **Cell culture and transfections.** Parasites were cultured in RPMI medium
317 supplemented with Albumax I (Gibco) and transfected as described earlier (37, 38). For
318 generation of *PfHsp70x-DDD* parasites, PfHsp70x-HADB was transfected in duplicates
319 into 3D7-derived parental strain PM1KO which contains a *hDHFR* expression cassette
320 conferring resistance to TMP (39). Selection and drug cycling were performed as
321 described (25) in the presence of 10 μM of TMP (Sigma). Integration was detected after
322 three rounds of drug cycling with blasticidin (Sigma).
323
324 For generation of PfHsp70x-*glmS* and PfHsp70x-*M9* parasites, a mix of three plasmids
325 (40 µg of each) was transfected in duplicates into 3D7 parasites. The plasmids mix
326 contained pUF1-Cas9 (from J. J. Lopez-Rubio, (30)) which contains the *DHOD*
327 resistance gene, pMK-U6-PfHsp70x, pHA-glmS-PfHsp70x or pHA-M9-PfHsp70x, which
328 are all marker-free. Drug pressure was applied 48 hours post transfection, using 1μM
329 DSM (40), selecting only for Cas9 expression. Drug was removed from the culturing
330 media once parasites became detectable in the culture, usually around 3 weeks post
331 transfection.
332
333 For generation of PfHsp70x-KO parasites, a mix of pUF1-Cas9 (from J. J. Lopez-Rubio,
334 (30)) and pL7-PfHsp70x (50 µg of each plasmid) was transfected in duplicates into 3D7

335 parasites. Drug pressure was applied 48 hours post transfection, using 2.5nM
336 WR99210 (Sigma), selecting for integration of the drug resistance cassette into the
337 *pfhsp70x* gene.
338
339 **Growth assays.** For asynchronous growth assays of PfHsp70x-DDD lines, parasites
340 were washed twice and incubated without TMP. For asynchronous growth assays of
341 PfHsp70x-*glmS* and PfHsp70x-*M9 parasites*, 5 or 10 mM GlcN (Sigma) were added to
342 the growth media. Asynchronous growth assays of PfHsp70x-KO parasites were
343 performed in media containing WR99210. Parasitemia was monitored every 24 hours
344 via flow cytometry. For flow cytometry, aliquots of parasite cultures (5 μl) were stained
345 with 1.5 mg/ml Acridine Orange (Molecular Probes) in PBS. The fluorescence profiles of
346 infected erythrocytes were measured by flow cytometry on a CyAn ADP (Beckman
347 Coulter) or CytoFLEX (Beckman Coulter) and analyzed by FlowJo software (Treestar,
348 Inc.). Whenever required, parasites were sub-cultured to avoid high parasite density
349 and relative parasitemia at each time point was back-calculated based on actual
350 parasitemia multiplied by the relevant dilution factors. 100% parasitemia was
351 determined as the highest relative parasitemia and was used to normalize parasite
352 growth. Data were fit to exponential growth equations using Prism (GraphPad Software,
353 Inc.)
354
355 **Southern blotting.** Southern blots were performed with genomic DNA isolated using
356 the Qiagen Blood and Cell Culture kit. 10 μg of DNA was digested overnight with
357 NcoI/XmnI for PfHsp70x-DDD and BamHI/ScaI for PfHsp70x-KO (New England

358 Biolabs). Integrants were screened using biotin-labeled probes against the 3'-end
359 (PfHsp70x-DDD parasites) or 5'-end (PfHsp70x-KO parasites) of the *pfhsp70x* ORF.
360 Southern blot was performed as described earlier (41). The probe was labeled using
361 biotinylated Biotin-16-dUTP (Sigma). The biotinylated probe was detected on blots
362 using IRDye 800CW Streptavidin conjugated dye (LICOR Biosciences) and was
363 imaged, processed and analyzed using the Odyssey infrared imaging system software
364 (LICOR Biosciences).
365
366 **Western blotting.** Western blots were performed as described previously (27). Briefly,
367 late-stage parasites were isolated on a percoll gradient (Genesee Scientific). For
368 PfHsp70x-DDD parasites, host RBCs were permeabilized selectively by treatment with
369 ice-cold 0.04% saponin in PBS for 10 min. Supernatants were collected for detection of
370 exported parasites proteins and pellets were collected for detection of proteins with the
371 parasite. For PfHsp70x-KO, PfHsp70x-*glmS* and PfHsp70x-*M9* parasites, whole
372 parasite lysates, including the host RBC, were used to detect protein expression and
373 export. The antibodies used in this study were rat anti-HA (3F10, Roche, 1:3000), rabbit
374 anti-PfEF1α (from D. Goldberg, 1: 2000), mouse anti-Plasmepsin V (From D. Goldberg,
375 1:400), rabbit anti-PfHsp70x (From J. Przyborski, 1:1000). The secondary antibodies
376 that were used are IRDye 680CW goat anti-rabbit IgG and IRDye 800CW goat anti-
377 mouse IgG (LICOR Biosciences, 1:20,000). The western blot images were processed
378 and analyzed using the Odyssey infrared imaging system software (LICOR
379 Biosciences).
380

381 **Microscopy and image processing.** For detection of HA-tags, PfHsp70x, PfFIKK4.2,
382 and MAHRP1, cells were smeared on a slide and acetone-fixed. For KAHRP detection,
383 cells were fixed with paraformaldehyde and glutaraldehyde. PfHsp70x-HA was detected
384 using rat anti-HA antibody (clone 3F10, Roche, 1:100). MAHRP1 was detected using
385 rabbit anti-MAHRP1 (from Hans-Peter Beck, 1:500). PfFIKK4.2 and KAHRP were
386 detected using mouse anti-PfFIKK4.2 (1:1000) and mouse anti-KAHRP (1:1000 and
387 1:500, respectively. Both antibodies acquired from David Cavanagh and EMRR).
388 Secondary antibodies used were anti rat-AlexaFluor 488 or 594, anti rabbit-AlexaFluor
389 488, and anti mouse-AlexaFluor 488 (Life Technologies, 1:100). Cells were mounted on
390 ProLong Diamond with DAPI (Invitrogen) and were imaged using DeltaVision II
391 microscope system with an Olympus IX-71 inverted microscope using a 100X objective.
392 Image processing, analysis and display were preformed using SoftWorx and Adobe
393 Photoshop. Adjustments to brightness and contrast were made for display purposes.
394

395 **Acknowledgments**

396 We thank Julie Nelson at the Center for Tropical and Emerging Global Diseases
397 Cytometry Shared Resource Laboratory; Muthugapatti Kandasamy at the University of
398 Georgia Biomedical Microscopy Core; Heather M. Bishop for technical assistance;
399 Jose-Juan Lopez-Rubio for sharing the pUF1-Cas9 and pL6 plasmids; and Dan
400 Goldberg (for anti-Plasmepsin V and anti-EF1α), Hans-Peter Beck (for anti-MAHRP),
401 Jude Przyborski (for anti-PfHsp70x), and David Cavanagh and EMRR (for anti-FIKK4.2
402 and anti-KAHRP). This work was supported by grants from the March of Dimes

403 Foundation (Basil O'Connor Starter Scholar Research Award), and the US National
404 Institutes of Health (R00AI099156) to V.M.
405

406 **References**

407 1. WHO. 2016. World Malaria ReportWorld Health Organization.
408 2. Cowman AF, Healer J, Marapana D, Marsh K. 2015. Malaria : Biology and
409 Disease. Cell 167:610–624.
410 3. Nilsson SK, Childs LM, Buckee C, Marti M. 2015. Targeting Human Transmission
411 Biology for Malaria Elimination. PLoS Pathog 11:e1004871.
412 4. Desai SA. 2014. Why do malaria parasites increase host erythrocyte
413 permeability? Trends Parasitol 30:151–159.
414 5. Maier AG, Cooke BM, Cowman AF, Tilley L. 2009. Malaria parasite proteins that
415 remodel the host erythrocyte. Nat Rev Microbiol 7:341–354.
416 6. Marti M, Good RT, Rug M, Knuepfer E, Cowman AF. 2004. Targeting Malaria
417 Virulence and Remodeling Proteins to the Host Erythrocyte. Science (80-)
418 306:1930–1933.
419 7. Hiller NL, Bhattacharjee S, Ooij C Van, Liolios K, Harrison T, Lopez-estran C,
420 Haldar K. 2004. A Host-Targeting Signal in Virulence Proteins Reveals a
421 Secretome in Malarial Infection. Science (80-) 306:1934–1937.
422 8. Klemba M, Goldberg DE. 2005. Characterization of plasmepsin V, a membrane-
423 bound aspartic protease homolog in the endoplasmic reticulum of Plasmodium
424 falciparum. Mol Biochem Parasitol 143:183–191.
425 9. Russo I, Babbitt S, Muralidharan V, Butler T, Oksman A, Goldberg DE. 2010.

426 Plasmepsin V licenses Plasmodium proteins for export into the host erythrocyte.
427 Nature 463:632–6.
428 10. Boddey J a, Hodder AN, Günther S, Gilson PR, Patsiouras H, Kapp E a, Pearce
429 JA, de Koning-Ward TF, Simpson RJ, Crabb BS, Cowman AF. 2010. An aspartyl
430 protease directs malaria effector proteins to the host cell. Nature 463:627–631.
431 11. Haase S, Herrmann S, Grüring C, Heiber A, Jansen PW, Langer C, Treeck M,
432 Cabrera A, Bruns C, Struck NS, Kono M, Engelberg K, Ruch U, Stunnenberg HG,
433 Gilberger TW, Spielmann T. 2009. Sequence requirements for the export of the
434 Plasmodium falciparum Maurer's clefts protein REX2. Mol Microbiol 71:1003–
435 1017.
436 12. Gruring C, Heiber A, Kruse F, Flemming S, Franci G, Colombo SF, Fasana E,
437 Schoeler H, Borgese N, Stunnenberg HG, Przyborski JM, Gilberger TW,
438 Spielmann T. 2012. Uncovering common principles in protein export of malaria
439 parasites. Cell Host Microbe 12:717–729.
440 13. de Koning-Ward TF, Gilson PR, Boddey JA, Rug M, Smith BJ, Papenfuss AT,
441 Sanders PR, Lundie RJ, Maier AG, Cowman AF, Crabb BS. 2009. A newly
442 discovered protein export machine in malaria parasites. Nature 459:945–9.
443 14. Gehde N, Hinrichs C, Montilla I, Charpian S, Lingelbach K, Przyborski JM. 2009.
444 Protein unfolding is an essential requirement for transport across the
445 parasitophorous vacuolar membrane of Plasmodium falciparum. Mol Microbiol
446 71:613–628.
447 15. Riglar DT, Rogers KL, Hanssen E, Turnbull L, Bullen HE, Charnaud SC,
448 Przyborski J, Gilson PR, Whitchurch CB, Crabb BS, Baum J, Cowman AF. 2013.

449 Spatial association with PTEX complexes defines regions for effector export into
450 Plasmodium falciparum-infected erythrocytes. Nat Commun 4:1415.
451 16. Boddey JA. 2014. Inhibition of Plasmepsin V activity demonstrates its essential
452 role in protein export, PfEMP1 display, and survival of malaria parasites. PLoS
453 Biol 12:e1001897.
454 17. Hodder AN, Sleebs BE, Czabotar PE, Gazdik M, Xu Y, O'Neill MT, Lopaticki S,
455 Nebl T, Triglia T, Smith BJ, Lowes K, Boddey JA, Cowman AF. 2015. Structural
456 basis for plasmepsin V inhibition that blocks export of malaria proteins to human
457 erythrocytes. Nat Struct Mol Biol 22:590–596.
458 18. Beck JR, Muralidharan V, Oksman A, Goldberg DE. 2014. PTEX component
459 HSP101 mediates export of diverse malaria effectors into host erythrocytes.
460 Nature 511:592–5.
461 19. Elsworth B, Matthews K, Nie CQ, Kalanon M, Charnaud SC, Sanders PR,
462 Chisholm SA, Counihan NA, Shaw PJ, Pino P, Chan J-A, Azevedo MF, Rogerson
463 SJ, Beeson JG, Crabb BS, Gilson PR, de Koning-Ward TF. 2014. PTEX is an
464 essential nexus for protein export in malaria parasites. Nature 511:587–91.
465 20. Maier AG, Rug M, O'Neill MT, Brown M, Chakravorty S, Szestak T, Chesson J,
466 Wu Y, Hughes K, Coppel RL, Newbold C, Beeson JG, Craig A, Crabb BS,
467 Cowman AF. 2008. Exported Proteins Required for Virulence and Rigidity of
468 Plasmodium falciparum-Infected Human Erythrocytes. Cell 134:48–61.
469 21. Külzer S, Charnaud S, Dagan T, Riedel J, Mandal P, Pesce ER, Blatch GL, Crabb
470 BS, Gilson PR, Przyborski JM. 2012. Plasmodium falciparum-encoded exported
471 hsp70/hsp40 chaperone/co-chaperone complexes within the host erythrocyte.

472 Cell Microbiol 14:1784–1795.
473 22. Rhiel M, Bittl V, Tribensky A, Charnaud SC, Strecker M, Müller S, Lanzer M,
474 Sanchez C, Schaeffer-Reiss C, Westermann B, Crabb BS, Gilson PR, Külzer S,
475 Przyborski JM. 2016. Trafficking of the exported P. falciparum chaperone
476 PfHsp70x. Sci Rep 6:36174.
477 23. Mesen-Ramirez P, Reinsch F, Blancke Soares A, Bergmann B, Ullrich AK, Tenzer
478 S, Spielmann T. 2016. Stable Translocation Intermediates Jam Global Protein
479 Export in Plasmodium falciparum Parasites and Link the PTEX Component EXP2
480 with Translocation Activity. PLoS Pathog 12:1–28.
481 24. Elsworth B, Sanders PR, Nebl T, Batinovic S, Kalanon M, Nie CQ, Charnaud SC,
482 Bullen HE, de Koning Ward TF, Tilley L, Crabb BS, Gilson PR. 2016. Proteomic
483 analysis reveals novel proteins associated with the Plasmodium protein exporter
484 PTEX and a loss of complex stability upon truncation of the core PTEX
485 component, PTEX150. Cell Microbiol.
486 25. Muralidharan V, Oksman A, Pal P, Lindquist S, Goldberg DE. 2012. Plasmodium
487 falciparum heat shock protein 110 stabilizes the asparagine repeat-rich parasite
488 proteome during malarial fevers. Nat Commun 3:1310.
489 26. Prommana P, Uthaipibull C, Wongsombat C, Kamchonwongpaisan S, Yuthavong
490 Y, Knuepfer E, Holder AA, Shaw PJ. 2013. Inducible Knockdown of Plasmodium
491 Gene Expression Using the glmS Ribozyme. PLoS One 8:1–10.
492 27. Muralidharan V, Oksman A, Iwamoto M, Wandless TJ, Goldberg DE. 2011.
493 Asparagine repeat function in a Plasmodium falciparum protein assessed via a
494 regulatable fluorescent affinity tag. Proc Natl Acad Sci U S A 108:4411–6.

495 28. Pei Y, Miller JL, Lindner SE, Vaughan AM, Torii M, Kappe SHI. 2013.
496 Plasmodium yoelii inhibitor of cysteine proteases is exported to exomembrane
497 structures and interacts with yoelipain-2 during asexual blood-stage development.
498 Cell Microbiol 15:1508–1526.
499 29. Nacer A, Claes A, Roberts A, Scheidig-Benatar C, Sakamoto H, Ghorbal M,
500 Lopez-Rubio J-J, Mattei D. 2015. Discovery of a novel and conserved
501 Plasmodium falciparum exported protein that is important for adhesion of PfEMP1
502 at the surface of infected erythrocytes. Cell Microbiol.
503 30. Ghorbal M, Gorman M, Macpherson CR, Martins RM, Scherf A, Lopez-Rubio J-J.
504 2014. Genome editing in the human malaria parasite Plasmodium falciparum
505 using the CRISPR-Cas9 system. Nat Biotechnol 32:819–21.
506 31. Kats LM, Fernandez KM, Glenister FK, Herrmann S, Buckingham DW, Siddiqui G,
507 Sharma L, Bamert R, Lucet I, Guillotte M, Mercereau-Puijalon O, Cooke BM.
508 2014. An exported kinase (FIKK4.2) that mediates virulence-associated changes
509 in Plasmodium falciparum-infected red blood cells. Int J Parasitol 44:319–328.
510 32. Watermeyer JM, Hale VL, Hackett F, Clare DK, Cutts EE, Vakonakis I, Fleck RA,
511 Blackman MJ, Saibil HR. 2016. A spiral scaffold underlies cytoadherent knobs in
512 Plasmodium falciparum-infected erythrocytes. Blood 127:343–51.
513 33. Spycher C, Rug M, Pachlatko E, Hanssen E, Ferguson D, Cowman AF, Tilley L,
514 Beck HP. 2008. The Maurer's cleft protein MAHRP1 is essential for trafficking of
515 PfEMP1 to the surface of Plasmodium falciparum-infected erythrocytes. Mol
516 Microbiol 68:1300–1314.
517 34. Pasini EME, Kirkegaard M, Mortensen P, Lutz HU, Thomas AW, Mann M. 2006.

518 In-depth analysis of the membrane and cytosolic proteome of red blood cells.
519 Blood 108:791–801.
520 35. Banumathy G, Singh V, Tatu U. 2002. Host chaperones are recruited in
521 membrane-bound complexes by Plasmodium falciparum. J Biol Chem 277:3902–
522 3912.
523 36. Egan ES, Jiang RHY, Moechtar MA, Barteneva NS, Weekes MP, Nobre L V, Gygi
524 SP, Paulo JA, Frantzreb C, Tani Y, Takahashi J, Watanabe S, Goldberg J, Paul
525 AS, Brugnara C, Root DE, Wiegand RC, Doench JG, Duraisingh MT. 2015. A
526 forward genetic screen identifies erythrocyte CD55 as essential for Plasmodium
527 falciparum invasion. Science 348:711–4.
528 37. Drew ME, Banerjee R, Uffman EW, Gilbertson S, Rosenthal PJ, Goldberg DE.
529 2008. Plasmodium food vacuole plasmepsins are activated by falcipains. J Biol
530 Chem 283:12870–12876.
531 38. Russo I, Oksman A, Goldberg DE. 2009. Fatty acid acylation regulates trafficking
532 of the unusual Plasmodium falciparum calpain to the nucleolus. Mol Microbiol
533 72:229–245.
534 39. Liu J, Gluzman IY, Drew ME, Goldberg DE. 2005. The role of Plasmodium
535 falciparum food vacuole plasmepsins. J Biol Chem 280:1432–1437.
536 40. Ganesan SM, Morrisey JM, Ke H, Painter HJ, Laroiya K, Phillips MA, Rathod PK,
537 Mather MW, Vaidya AB. 2011. Yeast dihydroorotate dehydrogenase as a new
538 selectable marker for Plasmodium falciparum transfection. Mol Biochem Parasitol
539 177:29–34.
540 41. Klemba M, Gluzman I, Goldberg DE. 2004. A Plasmodium falciparum dipeptidyl

541 aminopeptidase I participates in vacuolar hemoglobin degradation. J Biol Chem
542 279:43000–43007.
543

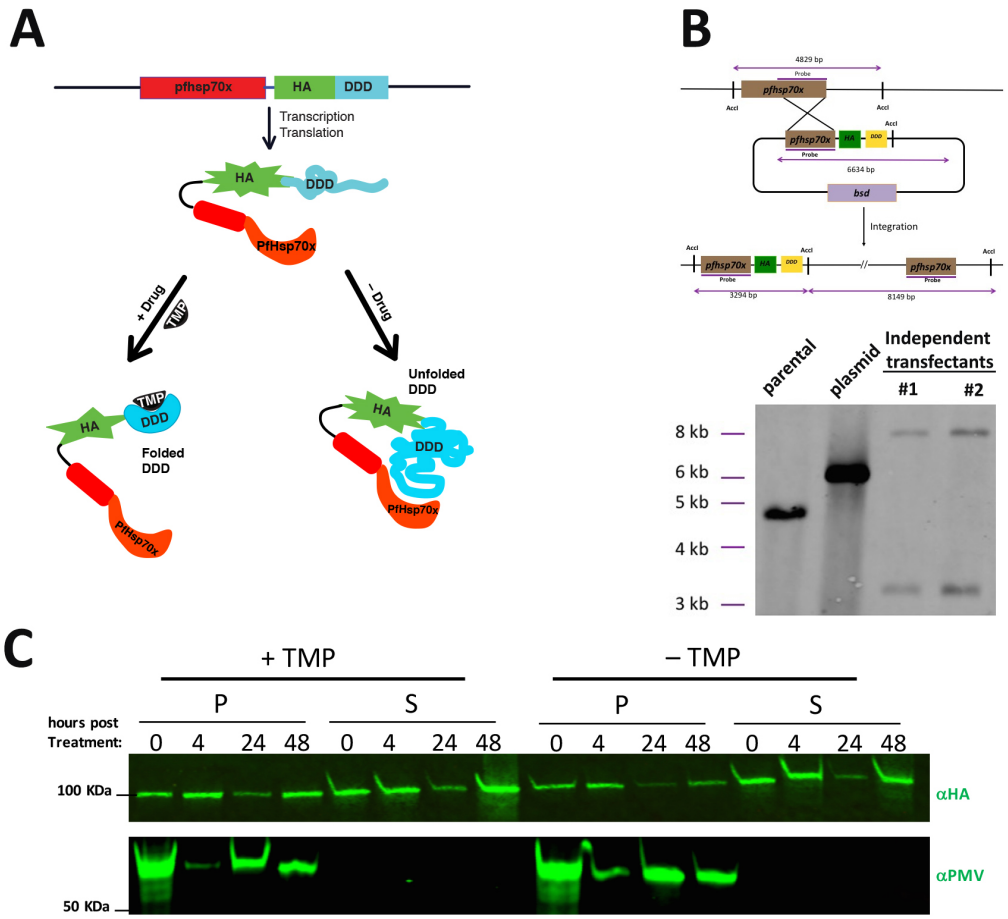
A
pfhsp70x
HA
DDD
Transcription
Translation
HA
DDD
PfHsp70x
+ Drug
TMP
– Drug
Unfolded
DDD
HA
DDD
PfHsp70x
TMP
HA
DDD
Folded
DDD
PfHsp70x
B
4829 bp
Probe
pfhsp70x
AccI
AccI
pfhsp70x
HA
DDD
Probe
6634 bp
bsd
Integration
AccI
AccI
AccI
pfhsp70x
HA
DDD
Probe
pfhsp70x
Probe
3294 bp
8149 bp
parental
plasmid
Independent
transfectants
#1
#2
8 kb
6 kb
5 kb
4 kb
3 kb
C
+ TMP
– TMP
P
S
P
S
hours post
Treatment:
0 4 24 48 0 4 24 48 0 4 24 48 0 4 24 48
100 KDa
αHA
50 KDa
αPMV

544

545

546

547 **Fig. 1. Generating PfHsp70x-DDD parasites.** (A) Mechanism of PfHsp70x-DDD
548 conditional inhibition. The *pfhsp70x* locus was modified to contain a triple hemagglutinin
549 (HA) tag and a DHFR-based destabilization domain (DDD). In the presence of
550 trimethoprim (TMP) the DDD is stable and the chaperone is active. Upon TMP removal
551 the chaperone binds the DDD intra-molecularly and cannot interact with client proteins,
552 inhibiting normal activity. (B) Single crossover homologous recombination enables the
553 integration of the plasmid into the 3' end of the *pfhsp70x* gene (upper panel). Southern
554 blot analysis of genomic DNA (bottom panel) isolated from parasite lines indicated
555 above the lanes. The genomic DNA was digested with AccI. Bands expected from
556 integration of the plasmid into the 3' end of the *pfhsp70x* gene were observed in two
557 independent transfections. A single band indicative of the parental allele was observed
558 for the parental strain and it was absent in the integrant parasites. (C) PfHsp70x-DDD
559 parasites were incubated without TMP, and Schizont stage parasites were purified on a
560 percoll gradient. Host cell lysates together with exported proteins were isolated using
561 0.04% cold saponin and were then collected from the supernatant (S). Parasites cells
562 with all non-exported proteins were collected from the pellet (P). Using western blot
563 analysis, the two fractions were analyzed and probed for PfHsp70x expression and
564 export. The membrane was probed with antibodies against HA (top) and Plasmepsin V
565 (loading control, bottom). The protein marker sizes that co-migrated with the probed
566 protein are shown on the left.
567

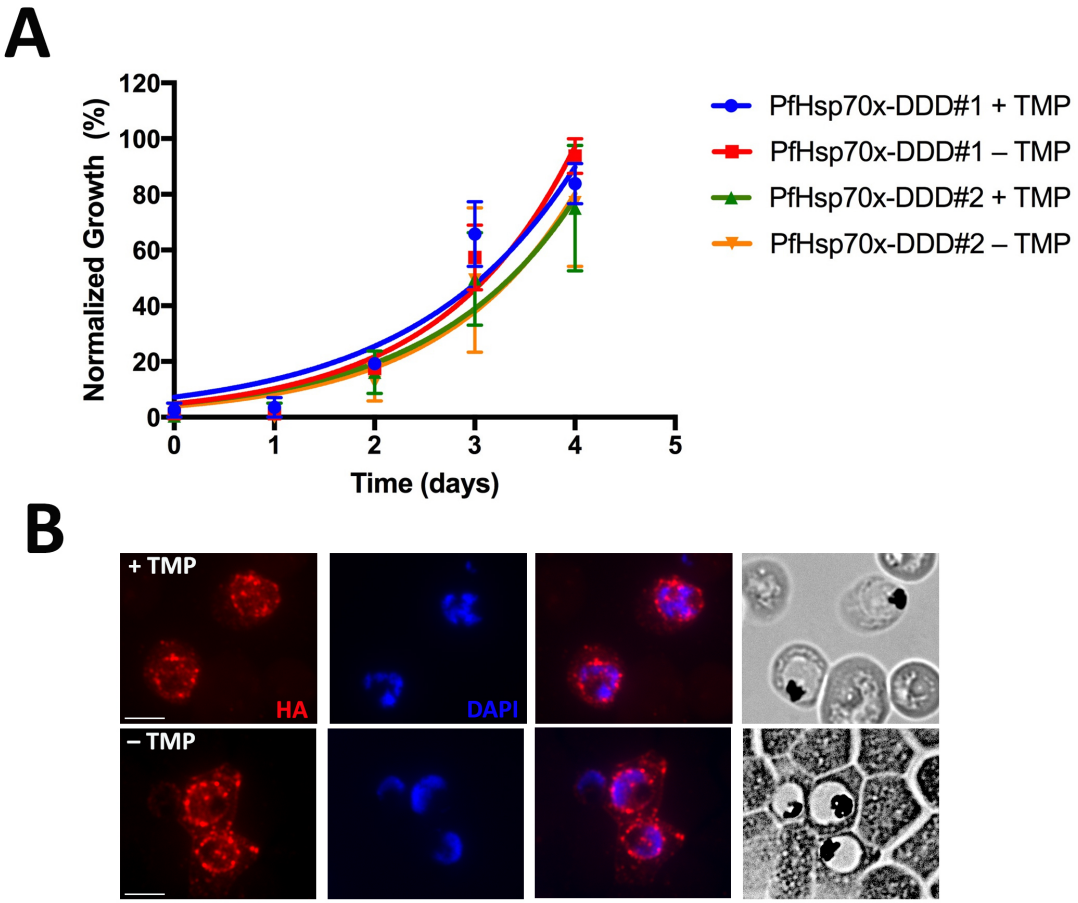
A
Normalized Growth (%)
120
100
80
60
40
20
0
0
1
2
3
4
5
Time (days)
PfHsp70x-DDD#1 + TMP
PfHsp70x-DDD#1 – TMP
PfHsp70x-DDD#2 + TMP
PfHsp70x-DDD#2 – TMP
B
+ TMP
HA
DAPI
– TMP

568

569

570 **Fig. 2. TMP removal does not affect parasite growth and PfHsp70x localization.**
571 (A) Asynchronous PfHsp70x-DDD parasites were grown with or without 10μM TMP and
572 parasitemia was monitored every 24 hours over 5 days. Data are fit to an exponential
573 growth equation and are represented as mean ± S.E.M. Experiments were done 3 times
574 and biological replicates are shown. (B) Immunofluorescence imaging of acetone fixed
575 PfHsp70x-DDD parasites stained with antibodies against HA (green) and DAPI (blue).
576 Scale bar, 5μm.
577

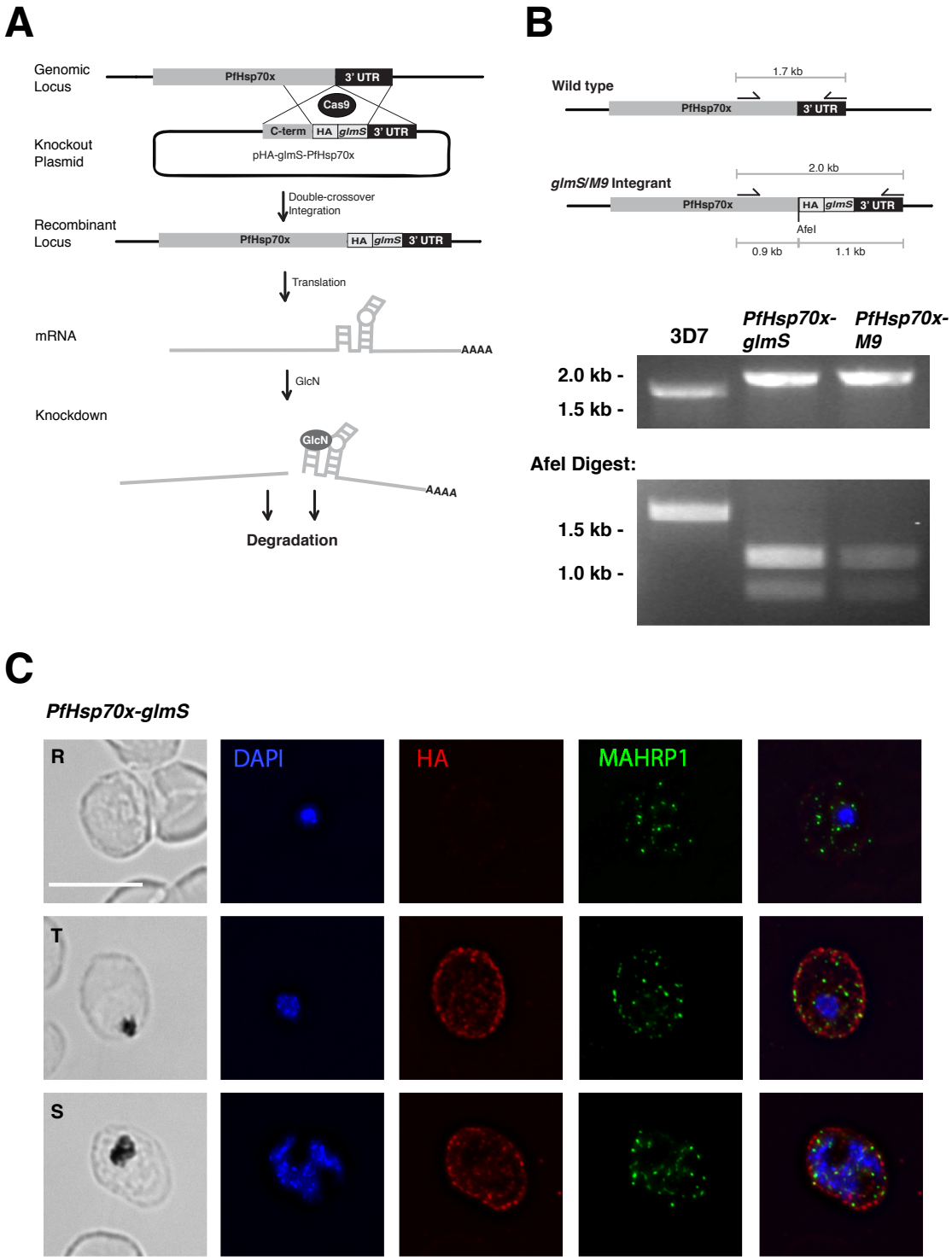
A
Genomic Locus
PfHsp70x
3' UTR
Cas9
C-term
HA
glmS
3' UTR
Knockout Plasmid
pHA-glmS-PfHsp70x
Double-crossover Integration
Recombinant Locus
PfHsp70x
HA
glmS
3' UTR
Translation
mRNA
AAAA
GlcN
Knockdown
GlcN
AAAA
Degradation
B
Wild type
1.7 kb
PfHsp70x
3' UTR
glmS/M9 Integrant
2.0 kb
PfHsp70x
HA
glmS
3' UTR
AfeI
0.9 kb
1.1 kb
3D7
PfHsp70x-glmS
PfHsp70x-M9
2.0 kb -
1.5 kb -
AfeI Digest:
1.5 kb -
1.0 kb -
C
PfHsp70x-glmS
R
T
S
DAPI
HA
MAHRP1

578

579

580 **Fig. 3. CRISPR/Cas9-mediated integration of HA-*glmS*/*M9* at PfHsp70x locus.**
581 (A) Diagram showing integration of 3xHA-ribozyme sequence and GlcN-induced
582 degradation of mRNA. Cas9 introduces a double-stranded break at the beginning of the
583 3' UTR of the *pfhsp70x* locus. The repair plasmid provides homology regions for double-
584 crossover homologous recombination, introducing a 3xHA tag and the ribozyme
585 sequence. Following translation and addition of GlcN, the PfHsp70x-*glmS* mRNA is
586 cleaved by the ribozyme and is subject to degradation. (B) PCR test confirming
587 integration at the PfHsp70x locus. DNA was purified from transfected, cloned parasites
588 and primers were used to amplify the region between the C-terminus and 3'UTR of
589 *pfhsp70x*. The PCR products were digested with AfeI, further confirming integration. (C)
590 IFA showing export of HA-tagged PfHsp70x. Asynchronous PfHsp70x-*glmS* parasites
591 were fixed with acetone and stained with specific antibodies. Images from left to right
592 are phase, DAPI (parasite nucleus, blue), anti-HA (red), anti-MAHRP1 (green), and
593 fluorescence merge. Scale bar represents 5 μm. (R) rings, (T) trophs and (S) schizont.
594

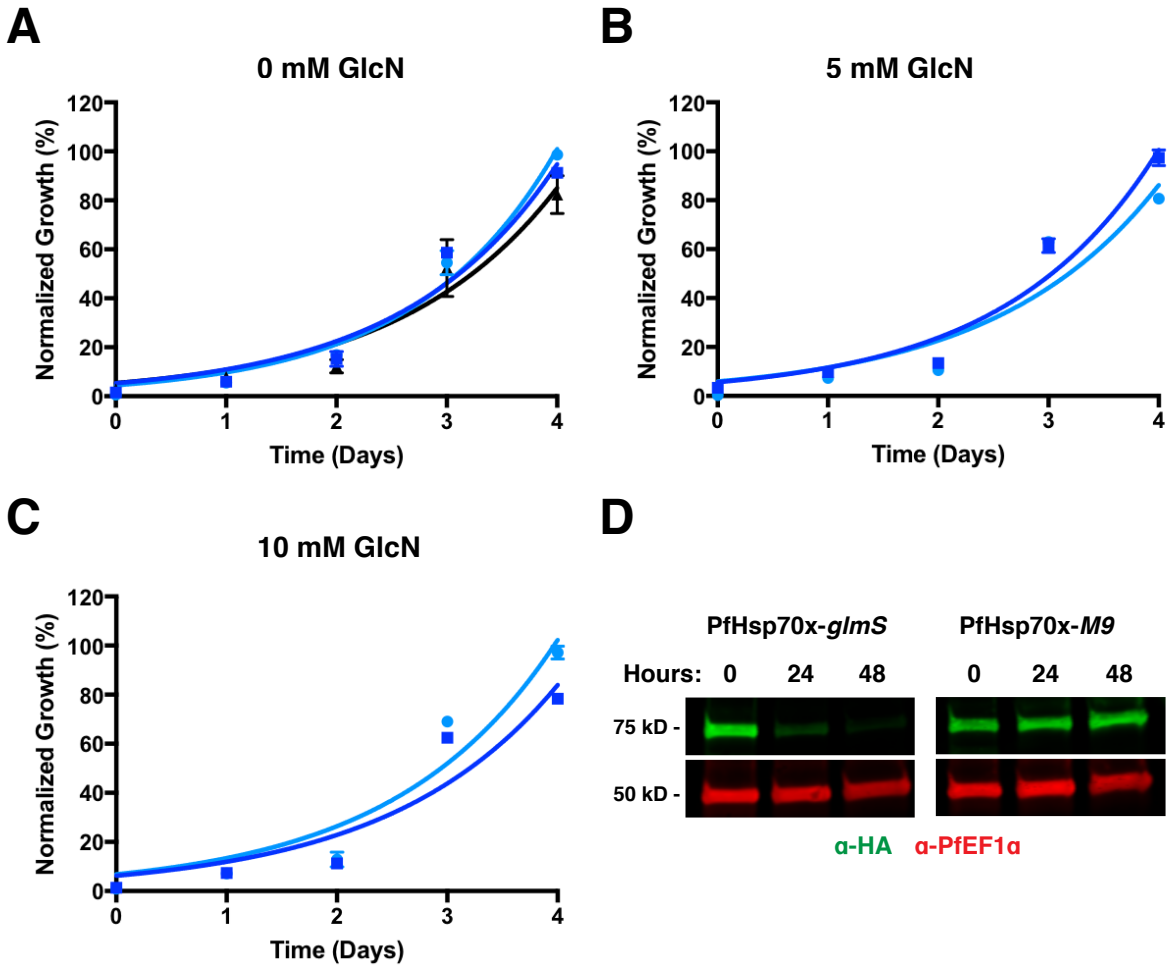
A
0 mM GlcN
Normalized Growth (%)
Time (Days)
B
5 mM GlcN
Normalized Growth (%)
Time (Days)
C
10 mM GlcN
Normalized Growth (%)
Time (Days)
D
PfHsp70x-glmS
PfHsp70x-M9
Hours: 0 24 48
0 24 48
75 kD -
50 kD -
α-HA
α-PfEF1α

595

596

597 **Fig. 4. GlcN-induced knockdown of PfHsp70x does not affect intraerythrocytic**
598 **growth.** (A) PfHsp70x-*glmS*, PfHsp70x-*M9*, and 3D7 (parental line) were seeded at
599 equal parasitemia in triplicate and grown in normal culturing media (complete RPMI).
600 Parasitemia was measured every 24 hours using flow cytometry. Data are fit to an
601 exponential growth equation and are represented as mean ± S.E.M. (n=3). (B) and (C)
602 PfHsp70x-*glmS* and PfHsp70x-*M9* parasites were seeded at equal parasitemia in
603 triplicate. Cultures were grown in the presence of either 5 (B) or 10 mM (C) GlcN.
604 Parasitemia was measured every 24 hours using flow cytometry. Data are fit to an
605 exponential growth equation and are represented as mean ± S.E.M. (n=3). (D)
606 PfHsp70x-*glmS* and PfHsp70x-*M9* parasites were grown in the presence of 7.5 mM
607 GlcN. Schizont-stage parasites were Percoll-purified every 24 hours, and whole parasite
608 lysates were used for western blot analysis. Membrane was probed with anti-HA, and
609 anti-PfEF1α (loading control).
610

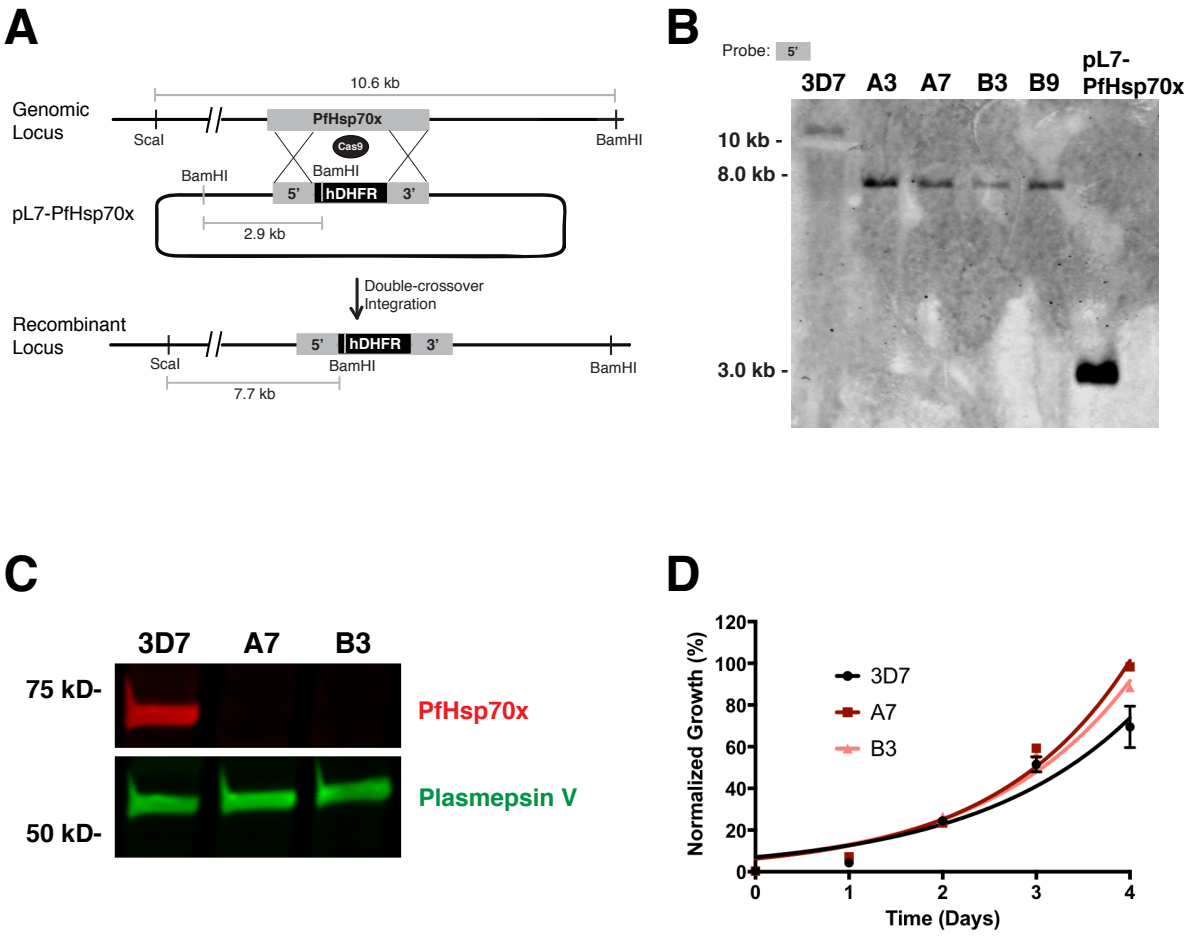
A
Genomic Locus
10.6 kb
PfHsp70x
ScaI
BamHI
Cas9
BamHI
BamHI
5'
hDHFR
3'
pL7-PfHsp70x
2.9 kb
Double-crossover Integration
Recombinant Locus
5'
hDHFR
3'
ScaI
BamHI
BamHI
7.7 kb
B
Probe: 5'
3D7
A3
A7
B3
B9
pL7-PfHsp70x
10 kb -
8.0 kb -
3.0 kb -
C
3D7
A7
B3
75 kD-
PfHsp70x
50 kD-
Plasmepsin V
D
Normalized Growth (%)
120
100
80
60
40
20
0
3D7
A7
B3
0
1
2
3
4
Time (Days)

611

612

613 **Fig. 5. Knockout of *pfhsp70x* does not affect intraerythrocytic growth**. (A)
614 Schematic showing interruption of PfHsp70x ORF with *hDHFR* cassette. Cas9-
615 mediated double-stranded break in the *pfhsp70x* ORF is repaired using homology
616 regions on the template plasmid while inserting an *hDHFR* cassette into the locus. (B)
617 Southern blot analysis confirming knockout of PfHsp70x. Genomic DNA from
618 independent knockout clones (A3, A7, B3, and B9) was isolated and digested with
619 BamHI and ScaI. Membrane was hybridized with a biotin-labeled probe complementary
620 to the first 800 base pairs of the *pfhsp70x* ORF. (C) Western blot analysis
621 demonstrating loss of PfHsp70x protein expression in independent knockout clones.
622 Schizont-stage parasites were Percoll-purified, and whole cell lysate was used for
623 analysis. Membrane was probed with antibodies raised against PfHsp70x, and against
624 Plasmepsin V as a loading control. (D) Parental lines and independent PfHsp70x-KO
625 clones (A7 and B3) were seeded at equal parasitemia in triplicate. Parasitemia was
626 measured every 24 hours using flow cytometry. Data are fit to an exponential growth
627 equation and are represented as mean ± S.E.M. (n=3).
628

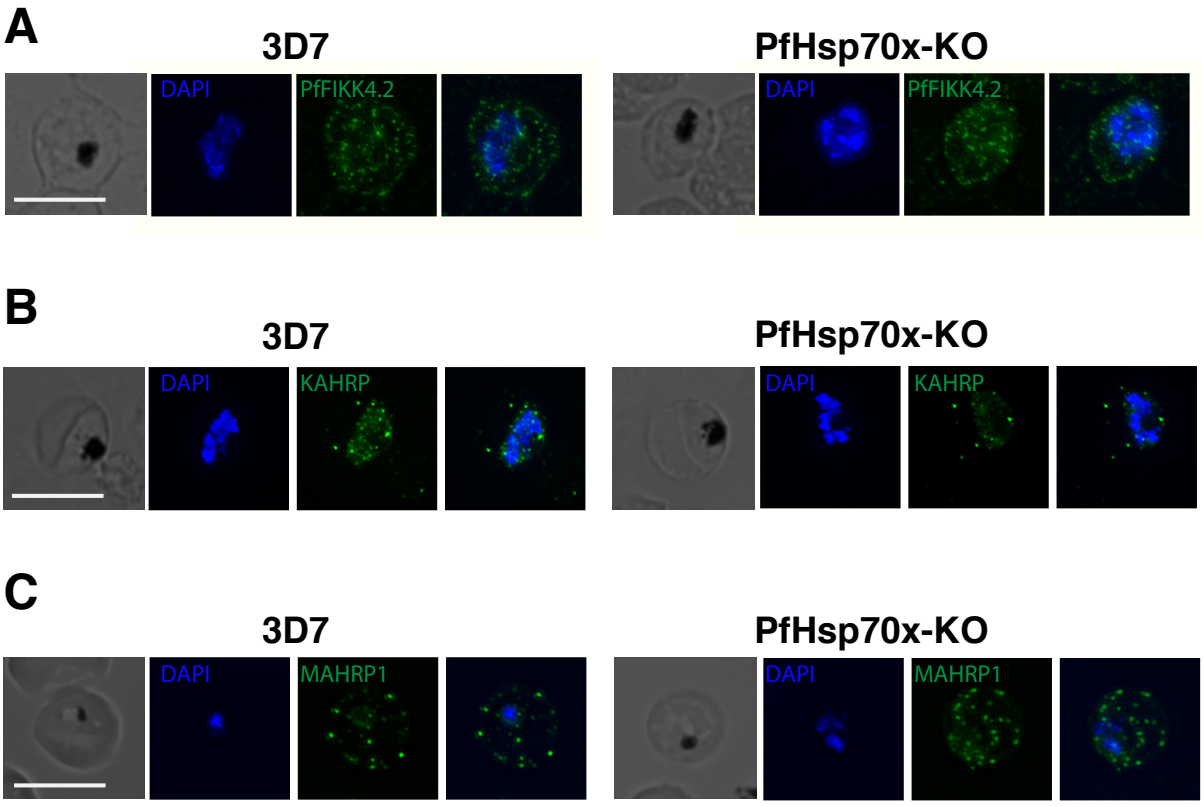
A
3D7
PfHsp70x-KO
DAPI
PfFIKK4.2
DAPI
PfFIKK4.2
B
3D7
PfHsp70x-KO
DAPI
KAHRP
DAPI
KAHRP
C
3D7
PfHsp70x-KO
DAPI
MAHRP1
DAPI
MAHRP1

629

630

631 **Fig. 6. PfHsp70x knockout does not inhibit export of virulence-associated**
632 **proteins**. Asynchronous 3D7 and PfHsp70x-KO parasites were fixed with acetone
633 (PfFIKK4.2 and MAHRP1) or paraformaldehyde (KAHRP) and stained with antibodies
634 against (A) PfFIKK4.2, (B) KAHRP, and (C) MAHRP1. DAPI used to mark parasite cell
635 nucleus. Images from left to right are phase, DAPI (blue), anti-exported protein (green),
636 and fluorescence merge. Scale bar represents 5μm. Representative images shown.
637